ELSEVIER

Sensors and Actuators A 69 (1998) 212–216

SENSORS AND ACTUATORS A PHYSICAL

An analytical analysis of a compressed bistable buckled beam

Mattias Vangbo [1]

Uppsala University, Ångström Laboratory, Department of Materials Science, Box 534, S-751 21 Uppsala, Sweden

Received 26 September 1997; received in revised form 5 February 1998

Abstract

A theoretical treatment to model the snap-through of a double-clamped beam is given. Starting from a classical theory for 'slender beams' the model is extended to also take compression into account. This significantly changes the predicted snap-through path, and may also change the snapping mechanism to a different regime where the maximum force is set by compression rather than the Euler instability. It is also shown that the model can be used for a class of non-homogeneous sandwich beams such as those micromachined in our referred experiment.

Keywords: Snap-through; Buckling; Bistable; Micromechanics; Snap-in holding structures

1. Introduction

Bistable structures are fundamental design elements, yet rarely found in micromechanics. They can be actuated into a position where they can exert a force without consuming power. Especially in the world of micromechanics, where powering is not trivial, and where it is not feasible to use alternatives such as bolts and nuts to fix things, monolithic bistable structures are of great need. The snap-through action of a buckled beam is an example of a bistable structure that will be focused on here. In a related work [1], we have fabricated similar devices and this paper intends to give an analytical comprehension of their properties and behaviour.

In e.g. micromechanics, monolithic designs and clamped configurations are preferred, but the snap action of the double-clamped beam specifically is rarely treated in the literature [2,3]. However, the snap-through of an arc, or 'oil-canning', is well investigated [4,5]. Furthermore, the influence of lateral compression of the beam due to the side wall pressure is often disregarded as small, and so the beam is considered as slender, but it will be shown below that such elastic deformations cannot always be neglected. In fact, depending on beam dimensions, the elastic energy can be arbitrarily distributed between bending and compression. The treatment below considers both the effects of bending and compression superimposed, but for comparison, calculations omitting the influence of compression will be plotted and referred to as the 'uncompensated model'. Dynamics will not be considered.

To adapt to the experimental conditions, the model is extended to include a class of non-homogeneous sandwich beam made up of a stiff core coated with a film with residual compressive stress (see Fig. 3). And because of aspects of application, a twin configuration, where two (or more) such beams are connected in parallel, is also considered. This will, as discussed later, defeat twisting during the snap.

2. Theory

2.1. Single beam

Fitting a beam of length $L+d$ ($d>0$), in a gap of width L will necessitate a curvature to the beam. Pushing the centre point of the buckled beam towards and past the middle will cause a so-called snap-through (see Fig. 1).

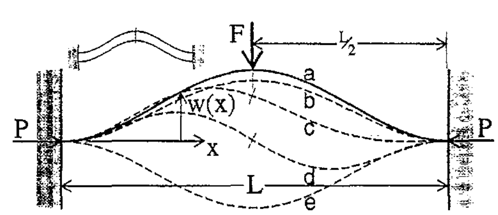

Fig. 1. Snap-through of a double-clamped single beam. Lines (a–e) indicate different stages during the snap due to the increasing force F. To illustrate how the centre point twists during the snap, its normal is also indicated. The two beams in the upper left corner shows the coupled configuration discussed in the text.

[1] Tel.: +46-18-471-30-15; fax: +46-18-55-50-95; e-mail: mattias.vangbo@angstrom.uu.se

0924-4247/98/$ - see front matter
PII S0924-4247(98)00097-1

This treatment of the snap-through behaviour has its origin in the theory of static Euler buckling of a double-clamped slender beam in its elastic region; see, e.g., the classical textbook by Timoshenko [6]. Additionally, the compressive action working on the beam as it is forced through the energy barrier is considered to overcome the restriction of slenderness otherwise assumed.

First consider the undisturbed case, i.e., $F=0$ (Fig. 1a). The equilibrium equation of an axially loaded beam is [6,7]

$$w^{(\mathrm{IV})}+n^2w''=0 \tag{1}$$

where $w=w(x)$ describes the centre line deflection of the beam, $n^2=P/EI_y$, and the boundary conditions are $w(0)=w'(0)=w(L)=w'(L)=0$ (P is the axial force, I_y is the beam's moment of inertia, and E is the Young's modulus). This is a homogeneous Sturm–Liouville problem, for which the eigenvalues n_iL are found to satisfy the equation

$$1-\cos(n_iL)=\tfrac{1}{2}n_iL\sin(n_iL) \tag{2}$$

The non-trivial eigenfunctions can be divided into two groups:
even solutions: $i=0, 2, 4, \ldots$, i.e. $n_iL=2\pi, 4\pi, 6\pi, \ldots$

$$w_i(x)=A_i[1-\cos(n_ix)] \tag{3}$$

and odd solutions: $i=1, 3, 5, \ldots$ i.e., $n_iL\approx 2.86\pi$, 4.92π, $6.94\pi, \ldots$

$$w_i(x)=A_i\left[1-\cos(n_ix)-\frac{2}{n_iL}(n_ix-\sin(n_ix))\right] \tag{4}$$

where A_i are arbitrary constants, i.e., the amplitudes of the functions. The ground state is represented by $i=0$ and $P_0=n_0{}^2EI_y$ is the force exerted on the boundary walls by the beam at this unperturbed mode of bending. The solutions $w_i(x)$ have the courtesy to be mutually orthogonal, and so are their respective first and second derivatives.

When applying a force, $F<0$ (as it is opposite to the deflection, w), our problem is to find a superposition $w(x)$ of the $w_i(x)$, that minimises the energy of the system under the constraint of a given length, $L+(d_0-d_P)$ of the beam. Here, d_0 is the excess length of the free uncompressed beam from which

$$d_P=PL/EA \tag{5}$$

i.e., the contraction from the side wall pressure, is subtracted. A is the cross-section area of the beam. In order to calculate the length, we use the approximation:

$$L+d_0-d_P=\int_0^L\sqrt{1+[w'(x)]^2}\,\mathrm{d}x$$

$$\approx\int_0^L\left\{1+\frac{[w'(x)]^2}{2}\right\}\mathrm{d}x \tag{6}$$

and solving this integral gives us the constraint:

$$g(\bar{A})=(d_0-d_P)L-\sum_{i=0}^{\infty}\frac{A_i^2(n_iL)^2}{4}=0 \tag{7}$$

The energy of the system (neglecting the static d_0) can be written as:

$$U(\bar{A},F)=\frac{EI_y}{2}\int_0^L[w''(x)]^2\mathrm{d}x+Fw\left(\frac{L}{2}\right)+\frac{Pd_P}{2}$$

$$=\frac{EI_y}{2L^3}\sum_{i=0}^{\infty}A_i^2(n_iL)^4+2F\sum_{j=0}^{\infty}A_{4j}+\frac{Pd_P}{2} \tag{8}$$

where the first term is the energy associated with bending of the beam, and the second term is the potential energy of the load set at the centre of the beam. The third term develops as the beam is laterally compressed; the omission of this term is what will be referred to as the 'uncompensated model' below. A Lagrangian $\mathscr{L}$ with a Lagrange parameter, λ, is now introduced in order to find the equilibrium state for a constant F:

$$\mathscr{L}(U,\lambda)=U(\bar{A})+\lambda g(\bar{A}) \tag{9}$$

where

$$\frac{\partial\mathscr{L}}{\partial A_i}=0\left(\text{and }\frac{\partial\mathscr{L}}{\partial\lambda}=g(\bar{A})=0\right) \tag{10}$$

If $F=0$, Eq. (10) sets all but one A_i to zero and leaves the last A_i non-zero (to satisfy Eq. (7)) only if λ is set to a corresponding discrete value,

$$\lambda_i=(n_iL)^2\frac{EI_y}{L^3}=\frac{P_i}{L} \tag{11}$$

This represents one regular mode of Euler buckling (note that only the first mode, $i=0$, is stable), and by inserting the expression for n_i, λ_iL turns out to be equal to the axial force P_i.

If $F\neq 0$ the A_i involved in the potential energy term of Eq. (8) are non-zero. From Eq. (10):

$$\begin{cases}A_i(F)=\dfrac{4FL^3}{EI_y(n_iL)^2((\eta L)^2-(n_iL)^2)} & i=0, 4, 8, \ldots\\[2ex] A_i=0 & \text{otherwise}\end{cases} \tag{12}$$

where

$$\eta^2=\frac{P}{EI_y} \tag{13}$$

Here the free parameter η is distinguished from n solving Eq. (1); however, they are identically defined. These A_i inserted into the boundary condition (7) will, together with a summation of the centre point deflections of the different modes, yield the total centre point deflection as a function of force

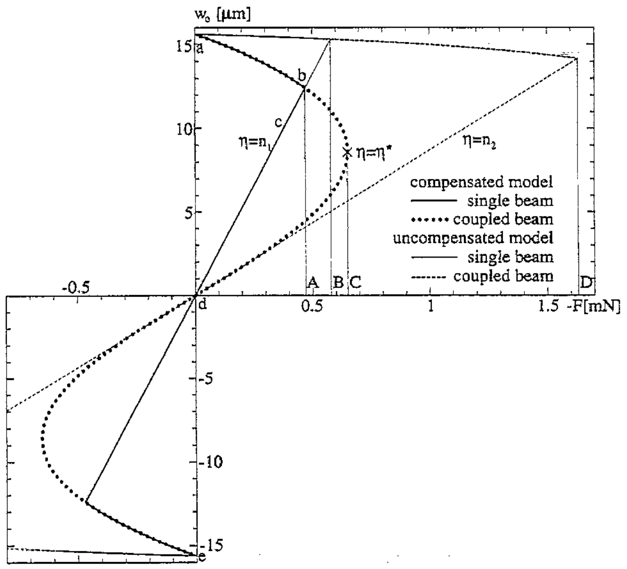

Fig. 2. The characteristics of the compensated and uncompensated models for both single and coupled beams. Letters (a–e) correspond to Fig. 1, where the shape of the beam is drawn at the indicated stages during the snap through. The maximum forces along the different paths are indexed (A–D).

on a parametric form (see Fig. 2 which, for symmetry reasons, is drawn on both sides of the origon):

$$\begin{aligned} F(\eta) &= -\frac{EI_y}{2L^3}\sqrt{[d_0-d_P(\eta)]L} \\ &\quad\times\left[\sum_{j=0}^{\infty}\frac{1}{(n_{4j}L)^2((\eta L)^2-(n_{4j}L)^2)}\right]^{-1/2} \\ &= -\frac{4(\eta L)^2 EI_y}{L^3}\sqrt{(d_0-d_P(\eta))L} \\ &\quad\times\left[3-\frac{3}{\eta L}\tan\left(\frac{\eta L}{4}\right)+\tan^2\left(\frac{\eta L}{4}\right)\right]^{-1/2} \end{aligned} \tag{14}$$

$$\begin{aligned} w(\eta) &= 2\sum_{j=0}^{\infty}A_{4j} \\ &= -\frac{8L^3}{EI_y}F(\eta)\sum_{j=0}^{\infty}\frac{1}{(n_{4j}L)^2((\eta L)^2-(n_{4j}L)^2)} \\ &= -\frac{L^3}{(\eta L)^2 EI_y}F(\eta)\left[\frac{1}{4}-\frac{1}{\eta L}\tan\left(\frac{\eta L}{4}\right)\right] \\ &\xrightarrow{F\to 0}\frac{2}{\pi}\sqrt{(d_0-d_P(n_0))L} \end{aligned} \tag{15}$$

where $d_P(\eta)=(\eta L)^2 EI_y/LEA$, cf. Eqs. (5) and (13). The unperturbed centre point deflection at $F=0$ was calculated by letting $\eta\to n_0$. The equations also give us the spring constant, which varies along the path. At $F=0$, it has its largest value:

$$\left.\frac{\partial F/\partial\eta}{\partial w/\partial\eta}\right|_{F=0} = \frac{EI_y}{L^3}\left[\frac{10-\pi^2}{16\pi^4}+\frac{EI_y}{d_0\pi^2 LEA-4\pi^4 EI_y}\right]^{-1} < 11952\frac{EI_y}{L^3} \tag{16}$$

Notice here, that when we apply an increasing force F on the beam the axial force from the side walls must increase starting from P_0, but it cannot exceed P_1 since the beam will by means of developing the first mode wind itself through the energy barrier at this stage.[2]

When P_1 is reached, the corresponding buckling mode becomes possible, i.e., A_1 starts to increase according to the boundary condition (7) at the sacrifice of A_i; $i=0, 4, 8, \ldots$ that will start to decrease still according to Eq. (12). In this post-critical region, the parametric coupling is lost, and F is no longer a function of η. Instead, by inserting $\eta=n_1$ in Eq. (15), the force becomes directly proportional to the centre point deflection. Note that this 'spring constant' is negative:

$$\begin{aligned} w(F) &= 2\sum_{j=0}^{\infty}A_{4j} \\ &= -\frac{L^3}{(n_1 L)^2 EI_y}F\left[\frac{1}{4}-\frac{1}{n_1 L}\tan\left(\frac{n_1 L}{4}\right)\right] \\ &\approx -\frac{1}{207.7}\frac{L^3}{EI_y}F \end{aligned} \tag{17}$$

The maximum force needed to snap the beam is in most cases simply where the two cases (Eqs. (14) and (15)) and Eq. (17) intersect (see Fig. 2):

$$\begin{aligned} F(n_1) &= -\frac{EI_y}{L^3}\sqrt{(d_0-d_{P_1})L}(n_1 L)^3 \\ &\quad\times\left[1+\sqrt{(n_1 L/2)^2+1}\right]^{-1} \\ &\approx -129.5\frac{EI_y}{L^3}\sqrt{(d_0-d_{P_1})L} \end{aligned} \tag{18}$$

However, if the beam is a little stiff Eq. (14) has a maximum at $\eta^*<n_1$ and in that case $F(\eta^*)$ instead is the maximum force (in the case of coupled beams this effect will become significant, see below). To a good approximation (truncating the series expansion)

$$\eta^{*2}\approx\frac{2d_0 EA}{3LEI_y}+\frac{4\pi^2}{3L^2} \tag{19}$$

[2] Pulling the beam, on the other hand, i.e., $F>0$, will just lower the side wall pressure which, when going below zero, will become tensile and finally the beam will come to a failure. The formulas are valid in this form as long as $\lambda\geq 0$.

The activation energy is calculated from Eq. (8):

$$U_a=U(A_1,0)-U(A_0,0)=\frac{EI}{L^2}d_0[(n_1L)^2-(n_0L)^2]-\frac{(EI)^2}{2L^3EA}[(n_1L)^4-(n_0L)^4] \quad (20)$$

2.2. Coupled beam

As the single beam is snapped through an asymmetric mode, anything mounted on the centre point of the beam will make a twisted path (Fig. 1). To accommodate a linear movement, coupling of two or more equal beams in parallel (see Fig. 1) will effectively prevent the asymmetric modes from developing, i.e., by setting $w'(L/2)=0$.

The characteristics (per beam) initially do follow the same Eqs. (14)–(16), but as no asymmetric modes can develop, the critical point is postponed until $\eta=n_2$. The behaviour beyond the critical point is evaluated by replacing n_1 with n_2 in Eq. (17):

$$w(F)=-\frac{L^3}{(\eta_2L)^2EI_y}F\left[\frac{1}{4}-\frac{1}{n_2L}\tan\left(\frac{n_2L}{4}\right)\right]\approx-\frac{1}{631.7}\frac{L^3}{EI_y}F \quad (21)$$

In this post-critical region, the coupled beam is about three times as (inverse) stiff as the single beam. If $\eta^*>n_2$, the maximum force is (cf. Eq. (18)):

$$F(n_2)\approx-729.4\frac{EI_y}{L^3}\sqrt{(d_0-d_{P_2})L} \quad (22)$$

but in this coupled case, it is not very unlikely that a design would yield $\eta^*<n_2$; if so, the maximum force is set by $F(\eta^*)$ rather than $F(n_2)$. For the activation energy, Eq. (20) is used but with n_1 replaced by n_2.

2.3. Coated beam

Until now the beam has been considered homogeneous. However, to adapt the model to our needs [1], an extension to non-homogeneous beams will be made. In the general case, such beams would exhibit deformation due to shear stress but, in cases where the cross-section can be assumed to remain normal to the deflected beam axis, the classical bending theory used above still applies [6,8]. Consider a beam of length L, made from a stiff material such as silicon coated on all four sides with an oxide film of thickness t with a residual compressive stress (thus giving a stress distribution through the beam and accordingly a d_0, see Fig. 3). In this case, due to symmetry, such an assumption is adequate.

The momentum at a beam cross-section can be written:

$$M(x)=\int_{\text{cross-section}} z\sigma(x,y,z)\,\mathrm{d}y\,\mathrm{d}z \quad (23)$$

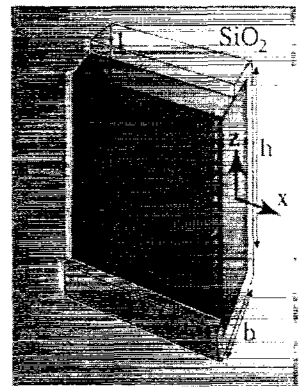

Fig. 3. Cross-section of the beam used in the referred experiment. The oxide film has a residual compressive stress.

where for a homogeneous beam $\sigma(x,y,z)=E[\varepsilon_P-w''(x)z]$, ε_P is the centre line strain due to the side wall pressure, so that

$$M(x)=-w''(x)EI_y \quad (24)$$

Momentum equilibrium $M''(x)=-Pw''(x)$ then gives Eq. (1) [6,7]. Coating the beam with a stressed film adds another contribution of stress, $\sigma_0(y,z)$,

$$\sigma(x,y,z)=E(y,z)[\varepsilon_P-w''(x)z]+\sigma_0(y,z) \quad (25)$$

Its shape of distribution is usually not predictable but assumed symmetric around $z=0$. Now solving the integral (23) again we get

$$M(x)=-w''(x)\left\{E_{\text{core}}\frac{hb^3}{12}+E_{\text{film}}\times\left[\frac{(h+2t)(b+2t)^3}{12}-\frac{hb^3}{12}\right]\right\}=-w''(x)[E_{\text{core}}I_{\text{core}}+E_{\text{film}}I_{\text{film}}] \quad (26)$$

and we can thus identify $[E_{\text{core}}I_{\text{core}}+E_{\text{film}}I_{\text{film}}]$ as an effective $(EI_y)_{\text{eff}}$ going into Eq. (1).

Similarly, as ε_P is equal in the core and in the film and the side wall pressure can be divided into

$$P=P_{\text{core}}+P_{\text{film}}=\varepsilon_PE_{\text{core}}A_{\text{core}}+\varepsilon_PE_{\text{film}}A_{\text{film}} \quad (27)$$

an effective $(EA)_{\text{eff}}=E_{\text{core}}A_{\text{core}}+E_{\text{film}}A_{\text{film}}$ can be identified. Note, however, that we choose not to calculate any effective E_{eff} or $(I_y)_{\text{eff}}$.

3. Results

The snap-through characteristics of a beam are exemplified by a 'quite slender' beam ($b=6.6$ μm, $h=28$ μm, $L=1000$ μm, and $t=1$ μm giving [1] an initial centre point deflection $w_0\approx15.8$ μm, $(EI_y)_{\text{eff}}\approx0.182$ μN/μm and $(EA)_{\text{eff}}\approx36.7$ N), but chosen so that $n_1<\eta^*<n_2$. In Fig. 2, the compensated and uncompensated models are compared for the single

and coupled beam configurations. Each of these four paths are made up from a curved part given by Eqs. (14) and (15), and a straight part, Eq. (17) or Eq. (21). The maximum force along the compensated path of the coupled configuration is marked '×' and note that it is, in this case, not where the two portions of the path meet and giving a maximum force of less that half of the uncompensated value.

Evaluating the bending and compression energy terms of Eq. (8) for this specific beam illustrates another interesting result. Starting from the ground state, the term for bending is larger but as η increases the elastic energy term increases rapidly, indicating that the beam is shortened. The term for bending then actually decreases and at about $\eta > n_1$ the elastic term is larger. Beyond the critical point, n_1 or n_2, the term for bending starts to increase again while that for the elastic remains constant due to a constant side wall pressure.

4. Discussion

As exemplified in Fig. 2, the compensated characteristics are confined 'inside' the uncompensated, always giving lower predicted maximum force and activation energy. Note the large difference of the predicted maximum forces between the compensated and uncompensated models for coupled beams (C vs. D), but also that the corresponding difference between the single and coupled configurations within the compensated model is moderate (A vs. C).

Not mentioned before, there is also a limit where the beam is just compressed rather than snapped through, i.e., the beam will never reach the critical point at all. This happens if $d_0 < d_{P_1}$ or in the case of a (homogeneous) rectangular beam cross-section if $d_0/L < \pi^2 b^2/3L^2$. The activation energy as given in Eq. (20) is not valid in this region, instead an approximation $U_a \approx (1/2) F_{\max} w(L/2)|_{F=0}$ may be used. However, the maximum force is still given by $F(\eta^*)$. Note that when passing the middle (origon), the beam is not buckled at all, so all energy is in the compression term of Eq. (8). This is, in some sense, the opposite extreme to the perfectly slender beam, where all energy goes into the bending term.

Still an expected discrepancy of the model from a true behaviour is the effect of quasi-buckling [9], which may enter under non-ideal circumstances, so that the initiation of a new buckling mode is not so distinct. It can thus be expected to 'round off' the shape of the characteristics at the critical point when the new mode is introduced.

5. Conclusions

It has been shown that the predicted snap-through characteristics may deviate severely from the classical uncompensated model even for 'quite slender' beams if contraction is taken into account. Depending on beam dimensions, there may also be a change in the snap-through mechanism, so that the maximum force is set by compression rather than by the instability. This especially applies for coupled configurations. In general, both the predicted maximum force to snap the beam and the activation energy are significantly lowered. This impacts both the dimensioning of devices to meet a given specification, i.e., to hold a certain load, and consequently dimensioning of the eventual actuator to control the beam. Minimising exaggerated dimensioning is important without exception for micromechanics, where a strong actuation is difficult.

Acknowledgements

I am indebted to Sten Herlitz for his knowledge in solid mechanics and I also thank my supervisors Professor Bertil Hök and Assistant Professor Ylva Bäcklund for their support.

References

[1] M. Vangbo, Y. Bäcklund, A bistable buckled beam, J. Micromech. Microeng. 8 (1998) 29–32.
[2] W.-Y. Tseng, J. Dugundji, Nonlinear vibrations of a buckled beam under harmonic excitation, J. Appl. Mechanics 38 (1971) 467–476.
[3] D.S. Popescu, T.S.J. Lammerink, Miko Elwenspoek, Buckled Membranes for Microstructures, Proc. of IEEE Micro Electro Mechanical Systems (MEMS-94) (Cat. No.94CH3404-1), IEEE, New York, NY, USA, 1994 (xiv + 360 pp.), pp. 188–192.
[4] G.J. Simitses, An Introduction to the Elastic Stability of Structures, Prentice-Hall, NJ, 1976 (xii + 253 pp.), pp. 34–38, pp. 189–191 with its references.
[5] S.P. Timoshenko, J.M. Gere, Theory of Elastic Stability, 2nd rev. edn., McGraw-Hill, New York, 1961 (xvi + 541 pp.), pp. 305–310.
[6] S.P. Timoshenko, J.M. Gere, Mechanics of Materials, 1st edn., Chap. 6, Van Nostrand-Reinhold, New York, 1972, xiv + 552 pp.
[7] S.P. Timoshenko, J.M. Gere, Theory of Elastic Stability, 2nd rev. edn., McGraw-Hill, New York, 1961 (xvi + 541 pp.), pp. 1–3.
[8] Z.P. Bazant, L. Cedolin, Stability of Structures, Oxford Univ. Press, Oxford, 1991 (xxiv + 984 pp.), pp. 30–31.
[9] J. Söderkvist, U. Lindberg, Characteristics of quasi buckling, Sensors and Materials 6 (1994) 293–309.

Biographies

Mattias Vangbo (born 1969) received his M.Sc. in Materials Physics in 1994 from Uppsala University, Sweden, after finishing his diploma work on sol–gel deposited optical waveguides at the Institute of Optical Research. He has since joined the Microstructure science and technology efforts at Uppsala University located in the Ångström Laboratory. His main work has been with regard to dry and wet chemical etching of silicon for applications such as precision mounting of optical devices.